To appear in *Journal of Computational Physics* in 1997.

Stability Analysis of a Galerkin/Runge-Kutta Navier-Stokes Discretisation on Unstructured Tetrahedral Grids

M. B. Giles
Oxford University Computing Laboratory
Numerical Analysis Group

This paper presents a timestep stability analysis for a class of discretisations applied to the linearised form of the Navier-Stokes equations on a 3D domain with periodic boundary conditions. Using a suitable definition of the 'perturbation energy' it is shown that the energy is monotonically decreasing for both the original p.d.e. and the semi-discrete system of o.d.e.'s arising from a Galerkin discretisation on a tetrahedral grid. Using recent theoretical results concerning algebraic and generalised stability, sufficient stability limits are obtained for both global and local timesteps for fully discrete algorithms using Runge-Kutta time integration.

Oxford University Computing Laboratory
Numerical Analysis Group
Wolfson Building
Parks Road
Oxford, England OX1 3QD
E-mail: giles@comlab.oxford.ac.uk

April, 1997

1 Introduction

One motivation for the analysis in this paper was the observation by Wigton of instabilities in Navier-Stokes calculations on structured grids [1]. It appeared that the instabilities might be connected to large variations in the level of turbulent viscosity arising quite properly in certain physical situations. A possible cause of the instability was thought to be the timestep definition which was based on Fourier stability theory assuming constant coefficients. Therefore, an objective of this analysis was to determine sufficient conditions for the stability of discretisations of the Navier-Stokes equations with nonuniform viscosity.

The second motivation was the requirement for timestep stability limits for viscous calculations on unstructured grids. Inviscid calculations are now being performed almost routinely on unstructured grids for complete aircraft geometries (e.g. [2, 3, 4, 5]). Using energy analysis methods, Giles developed sufficient global and local timestep stability limits for a Galerkin discretisation of the Euler equations on a tetrahedral grid with two particular Runge-Kutta time integration schemes [6]; this has been used on an *ad hoc* basis for calculations using other algorithms including various upwinding and numerical smoothing formulations [3, 5]. Through parallel computing and efficient multigrid algorithms for unstructured grids [5], there is now the computational power to perform extremely large Navier-Stokes calculations on unstructured grids, and so there is a need for the supporting numerical analysis to give accurate global and local timestep stability limits.

Fourier stability analysis can only be applied to linear finite difference equations with constant coefficients on structured grids, and so it is not appropriate for this application. There are two other well-documented stability analysis methods which can be used with linear discretisations with variable coefficients on unstructured grids. One is the energy method [7] which relies on the careful construction of a suitably defined 'energy' which can be proven to monotonically decrease. The difficulty is usually in constructing an appropriate definition for the energy, but when this method can be applied it is very powerful in giving a very strong form of stability. It is used in this paper to prove the stability of the original linearised form of the Navier-Stokes partial differential equations, and the semi-discretised system of coupled o.d.e.'s that is produced by the Galerkin spatial discretisation.

The other stability analysis technique involves consideration of the eigenvalues of the matrix representing the discretisation of the spatial differential operator. This leads to sufficient conditions for asymptotic stability, as $t \to \infty$ for unsteady calculations or as $n \to \infty$ for calculations using local timesteps. Unfortunately, there are well-documented examples such as the first order upwinding of the convection equation on a finite 1D domain (e.g. [8, 9, 10]) for which this is not a practical stability criterion because it allows an unacceptably large transient growth before the eventual exponential decay. The next section

reviews this theory showing that the problem of large transient growth can arise whenever the spatial discretisation matrix is non-normal. It then presents recent results on algebraic and generalised stability for such applications giving sufficient conditions for stability. It is these new stability conditions which are used to construct sufficient stability limits for the full Galerkin/Runge-Kutta Navier-Stokes discretisation.

The analysis is performed for linear perturbations to a steady flow in which all flow variables are uniform with the exception of the three viscosity coefficients, μ, the shear viscosity, λ, the second coefficient of viscosity, and k, the thermal diffusivity. This choice of model problem is critical in several ways. Although it is the linearisation of the laminar Navier-Stokes equations that is used, the viscosity coefficients can each be interpreted as the sum of the laminar value plus a turbulent value arising from some turbulence model. Accordingly, there is no assumption of any fixed relationship between the three quantities, either the Stokes hypothesis linking μ and λ, or the assumption of a constant Prandtl number linking μ and k. The uniformity of the other flow variables is essential for key parts of the analysis. However, a more fundamental aspect of the uniformity is that it gives a physical situation in which flow perturbations are naturally damped, and so the flow is stable. Therefore, an instability of the semi-discrete or fully discrete equations can be viewed justifiably as an incorrect behaviour. The timestep limit which gives the onset of this instability can then be defined as the maximum stable timestep. In contrast, if a vortex sheet were taken as the steady flow and then linear perturbations were analysed, it would be determined that both the analytic and discrete equations were unstable. Even worse, the timescale of the most unstable discrete mode would be proportional to Δx so that it would be impossible to distinguish between a 'numerical instability' and the natural Helmholtz instability of the vortex sheet. It would not therefore be possible to use this alternative model problem to make any deductions about stable timestep limits.

After the following section reviewing numerical stability theory, there are separate sections for the analysis of the differential, semi-discrete and fully discrete Navier-Stokes equations. To focus attention on the important features of the stability analysis, many of the supporting details are presented in the three appendices.

2 Review of stability theory for Runge-Kutta methods

Discretisation of the scalar o.d.e.

$$\frac{du}{dt} = \lambda u, \tag{2.1}$$

using an explicit Runge-Kutta method with timestep k yields a difference equation of the form

$$u^{(n+1)} = L(\lambda k)\, u^{(n)} \tag{2.2}$$

where $L(z)$ is a polynomial function of degree p

$$L(z) = \sum_{m=0}^{p} a_m z^m, \tag{2.3}$$

with $a_0 = a_1 = 1$, $a_p \neq 0$. Discrete solutions of this difference equation on a finite time interval $0 \leq t \leq t_0$ will converge to the analytic solution as $k \to 0$. In addition, the discretisation is said to be *absolutely stable* for a particular value of k if it does not allow exponentially growing solutions as $t \to \infty$; this is satisfied provided λk lies within the stability region S in the complex plane defined by

$$S = \{z : |L(z)| \leq 1\}\,. \tag{2.4}$$

Examples of stability regions for different polynomials are given in Appendix A.

Suppose now that a real square matrix C has a complete set of eigenvectors and can thus be diagonalised,

$$C = T \Lambda T^{-1}, \tag{2.5}$$

with Λ being the diagonal matrix of eigenvalues of C, and the columns of T being the associated eigenvectors. The Runge-Kutta discretisation of the coupled system of o.d.e.'s,

$$\frac{dU}{dt} = CU, \tag{2.6}$$

can be written as

$$U^{(n+1)} = L(kC)\, U^{(n)} = T\, L(k\Lambda)\, T^{-1}\, U^{(n)}, \tag{2.7}$$

since

$$C^m = \left(T \Lambda T^{-1}\right)^m = T \Lambda^m T^{-1}. \tag{2.8}$$

Hence

$$U^{(n)} = T\ \left(L(k\Lambda)\right)^n\ T^{-1}\, U^{(0)}. \tag{2.9}$$

The necessary and sufficient condition for absolute stability as $n \to \infty$, requiring that there are no discrete solutions which grow exponentially with n, is therefore that $|L(k\lambda)| \leq 1$, or equivalently $k\lambda$ lies in S, for all eigenvalues λ of C. If this condition is satisfied, then using L_2 vector and matrix norms it follows that

$$\|U^{(n)}\| \ \leq\ \|T\|\, \|L(k\Lambda)\|^n\, \|T^{-1}\|\, \|U^{(0)}\| \ \leq\ \kappa(T)\, \|U^{(0)}\|, \tag{2.10}$$

where $\kappa(T)$ is the condition number of the eigenvector matrix T.

If the matrix C is normal, meaning that it has an orthogonal set of eigenvectors, then the eigenvectors can be normalised so that $\kappa(T)=1$. In this case, $\|U^{(n)}\|$ is a non-increasing function of n and $\|U^{(n)}\|^2$ represents a non-increasing 'energy' which could be used in an energy stability analysis.

If C is not normal, then the growth in $\|U^{(n)}\|$ is bounded by the condition number of the eigenvector matrix, $\kappa(T)$. Unfortunately, this can be very large indeed, allowing a very large transient growth in the solution even when for each eigenvalue $k\lambda$ lies strictly inside the stability region S and so $\|U^{(n)}\|$ must eventually decay exponentially. This problem can be particularly acute when the matrix C comes from the spatial discretisation of a p.d.e. in which case there is then a family of discretisations arising from a sequence of computational grids of decreasing mesh spacing h. It is possible in such circumstances for the sequence of condition numbers $\kappa(T)$ to grow exponentially, with an exponent inversely proportional to the mesh spacing [8]. There are two practical consequences of this exponential growth. In applications concerned with the behaviour of the solution as $t\to\infty$, it produces an unacceptably large amplification of machine rounding errors in linear computations and complete failure of the discrete computation in nonlinear cases. In applications concerned with a finite time interval, $0\le t\le t_0$, it prevents convergence of the discrete solution to the analytic solution as $h, k\to 0$ except in certain exceptional situations using spectral spatial discretisations.

The stability of discretisations of systems of o.d.e.'s with non-normal matrices has been a major research topic in the numerical analysis community in recent years [8, 9, 11, 12, 13, 14, 15]; A recent review article by van Dorsselaer *et al* [10] provides an excellent overview of these and many other references. The application is often to families of non-normal matrices arising from spatial discretisations of p.d.e.'s. Ideally, one would hope to prove *strong stability*,

$$\|U^{(n)}\| \;\le\; \gamma\,\|U^{(0)}\|, \tag{2.11}$$

with γ being a constant which is not only independent of n but is also a uniform bound applying to all matrices in the family of spatial discretisations for different mesh spacings h but with the timestep k being a function of h. One reason why strong stability is very desirable is that the Lax Equivalence Theorem proves that it is a necessary and sufficient condition for convergence of discrete solutions to the analytic solution on a finite time interval for all possible initial data, provided that the discretisation of the p.d.e. is consistent for sufficiently smooth initial data [7].

At present, the conditions under which strong stability can be proved are too restrictive to be useful in practical computations. Instead, attention has focussed on weaker definitions of stability which are more easily achieved and are still useful for practical computations. The one that is used in this paper is *algebraic stability* [8, 11, 12] which allows a linear growth in the transient solution of the form

$$\|U^{(n)}\| \;\le\; \gamma\, n\,\|U^{(0)}\|, \tag{2.12}$$

where γ is again a uniform constant. A sufficient condition for algebraic stability is that

$$\tau(kC) \subset S, \tag{2.13}$$

where the numerical range $\tau(kC)$ is a subset of the complex domain defined by

$$\tau(kC) = \left\{ k \, \frac{W^* C W}{W^* W} : W \neq 0 \right\} \tag{2.14}$$

where W can be any non-zero complex vector of the required dimension and W^* is its Hermitian, the complex conjugate transpose. The proof of sufficiency is given by Lenferink and Spijker [12]. It proceeds in two parts, first showing that a certain resolvent condition is sufficient for algebraic stability, and then showing that this resolvent condition is satisfied if the numerical range lies inside S. Reddy and Trefethen [8] prove that the resolvent condition is necessary as well as sufficient for algebraic stability.

In related research, Kreiss and Wu [9] have defined *generalised stability* which is based on exponentially weighted integrals over time for a inhomogeneous difference equation with homogeneous initial conditions. A similar restriction on the numerical range provides a sufficient condition for generalised stability, however the theory at present applies only to discretisations of hyperbolic p.d.e.'s and so does not apply to the Navier-Stokes equations considered in this paper.

By considering W to be an eigenvector of C, it can be seen that $k\lambda \in \tau(kC)$ for each eigenvalue of C and so the requirement that $\tau(kC) \subset S$ is a tighter restriction on the maximum allowable timestep than asymptotic stability. In comparison to strong stability, algebraic stability allows greater growth in transients when considering the solution behaviour as $t \to \infty$. On the finite time interval, it can be shown that under some very mild technical conditions they are sufficient for convergence of discrete solutions to the analytic solution as $h, k \to 0$ provided the initial data is smooth and the discretisation is consistent. It thus appears that this stability definition is a useful tool in analysing numerical discretisations, but additional research is still required.

In the Navier-Stokes application in this paper we will need to consider a slight generalisation to a system of o.d.e.'s of the form

$$M \frac{dU}{dt} = CU, \tag{2.15}$$

in which M is a real symmetric positive-definite matrix. The 'energy' is defined as $U^* M U$ which suggests the definition of new variables,

$$W = M^{1/2} U, \tag{2.16}$$

so that $\|W\|^2 = U^* M U$. If M is diagonal then $M^{1/2}$ is the diagonal matrix whose elements are the positive square root of the corresponding elements of M. If M is not diagonal then $M^{1/2}$ is equal to $T^{-1} \Lambda^{1/2} T$ where Λ is the diagonal matrix of

eigenvalues of M and T is the corresponding matrix of orthonormal eigenvectors. $T^{-1}=T^*$ and hence both $M^{1/2}$ and $M^{-1/2}$ are symmetric and positive definite.

Under the change of variables, the system of o.d.e.'s becomes

$$\frac{dW}{dt} = M^{-1/2} C M^{-1/2}\, W, \tag{2.17}$$

which is algebraically stable provided $\tau(k\, M^{-1/2} C M^{-1/2}) \subset S$. If C is either symmetric or anti-symmetric then so too is $M^{-1/2} C M^{-1/2}$ because of the symmetry of $M^{-1/2}$. Therefore, as discussed earlier the condition that the numerical range lies inside S also ensures that the energy, $\|W\|^2 = U^* M U$, will be non-increasing.

3 Analytic equations

The starting point for the analysis is the nonlinear Navier-Stokes equations,

$$\frac{\partial U}{\partial t} + \frac{\partial F_x}{\partial x} + \frac{\partial F_y}{\partial y} + \frac{\partial F_z}{\partial z} = 0. \tag{3.1}$$

U is the vector of conservation variables $(\rho, \rho u, \rho v, \rho w, \rho E)^T$ and the flux terms are all defined in Appendix B together with the equation of state for an ideal gas and the definitions of the stress tensor and the viscous heat flux vector. The equations are to be solved on a unit cubic domain Ω with periodic boundary conditions. The choice of periodic b.c.'s avoids the complication of analysing the influence of different analytic and discrete boundary conditions [16, 17].

The first step is to linearise the Navier-Stokes equations by considering perturbations to a steady flow which is uniform apart from spatial variations in the viscosity parameters μ, λ, k. Perturbations to the conserved variables are then related to the symmetrising variables of Gustafsson and Sundstrom [16] and Abarbanel and Gottlieb [18], by the equation

$$\widetilde{U} = S\, W. \tag{3.2}$$

The uniform transformation matrix S is given in Appendix B. Together, the linearisation and the change of variables yields an equation of the form

$$\begin{aligned} \frac{\partial W}{\partial t} + A_x \frac{\partial W}{\partial x} + A_y \frac{\partial W}{\partial y} + A_z \frac{\partial W}{\partial z} \;=\; & \frac{\partial}{\partial x}\left(D_{xx}\frac{\partial W}{\partial x} + D_{xy}\frac{\partial W}{\partial y} + D_{xz}\frac{\partial W}{\partial z}\right) \\ + \; & \frac{\partial}{\partial y}\left(D_{yx}\frac{\partial W}{\partial x} + D_{yy}\frac{\partial W}{\partial y} + D_{yz}\frac{\partial W}{\partial z}\right) \\ + \; & \frac{\partial}{\partial z}\left(D_{zx}\frac{\partial W}{\partial x} + D_{zy}\frac{\partial W}{\partial y} + D_{zz}\frac{\partial W}{\partial z}\right), \end{aligned} \tag{3.3}$$

in which the matrices A_x, A_y, A_z and the combined dissipation matrix

$$\begin{pmatrix} D_{xx} & D_{xy} & D_{xz} \\ D_{yx} & D_{yy} & D_{yz} \\ D_{zx} & D_{zy} & D_{zz} \end{pmatrix}$$

are all symmetric. The matrices are listed in detail in Appendix B and it is also proved that the combined dissipation matrix is positive semi–definite provided that $\mu \geq 0$, $2\mu+3\lambda \geq 0$ and $k \geq 0$. These three conditions are satisfied by the laminar viscosity coefficients; it will be assumed that they are also satisfied by the coefficients defined by the turbulence modelling.

The perturbation 'energy' is defined as

$$E = \int_\Omega \tfrac{1}{2} W^* W \, dV, \tag{3.4}$$

where W^* again denotes the Hermitian of W, and its rate of change is

$$\frac{dE}{dt} = \int_\Omega \tfrac{1}{2} \left(W^* \frac{\partial W}{\partial t} + \frac{\partial W^*}{\partial t} W \right) dV = \int_\Omega \tfrac{1}{2} \left(W^* \frac{\partial W}{\partial t} + \left(W^* \frac{\partial W}{\partial t} \right)^* \right) dV. \tag{3.5}$$

Using the fact that A_x is real and symmetric, and then integrating by parts using the periodic boundary conditions,

$$\begin{aligned} \int_\Omega \left(W^* A_x \frac{\partial W}{\partial x} \right)^* dV \;&=\; \int_\Omega \frac{\partial W^*}{\partial x} A_x W \, dV \;=\; -\int_\Omega W^* A_x \frac{\partial W}{\partial x} \, dV \\ \implies \qquad & \int_\Omega W^* A_x \frac{\partial W}{\partial x} + \left(W^* A_x \frac{\partial W}{\partial x} \right)^* dV = 0. \end{aligned} \tag{3.6}$$

Similarly,

$$\begin{aligned} \int_\Omega W^* A_y \frac{\partial W}{\partial y} + \left(W^* A_y \frac{\partial W}{\partial y} \right)^* dV \;&=\; 0, \\ \int_\Omega W^* A_z \frac{\partial W}{\partial z} + \left(W^* A_z \frac{\partial W}{\partial z} \right)^* dV \;&=\; 0. \end{aligned} \tag{3.7}$$

Integrating the diffusion terms by parts and noting that

$$\left[\begin{pmatrix} \frac{\partial W}{\partial x} \\ \frac{\partial W}{\partial y} \\ \frac{\partial W}{\partial z} \end{pmatrix}^* \begin{pmatrix} D_{xx} & D_{xy} & D_{xz} \\ D_{yx} & D_{yy} & D_{yz} \\ D_{zx} & D_{zy} & D_{zz} \end{pmatrix} \begin{pmatrix} \frac{\partial W}{\partial x} \\ \frac{\partial W}{\partial y} \\ \frac{\partial W}{\partial z} \end{pmatrix} \right]^* = \begin{pmatrix} \frac{\partial W}{\partial x} \\ \frac{\partial W}{\partial y} \\ \frac{\partial W}{\partial z} \end{pmatrix}^* \begin{pmatrix} D_{xx} & D_{xy} & D_{xz} \\ D_{yx} & D_{yy} & D_{yz} \\ D_{zx} & D_{zy} & D_{zz} \end{pmatrix} \begin{pmatrix} \frac{\partial W}{\partial x} \\ \frac{\partial W}{\partial y} \\ \frac{\partial W}{\partial z} \end{pmatrix} \tag{3.8}$$

since the combined dissipation matrix is real and symmetric, yields the final result,

$$\frac{dE}{dt} = -\int_\Omega \begin{pmatrix} \frac{\partial W}{\partial x} \\ \frac{\partial W}{\partial y} \\ \frac{\partial W}{\partial z} \end{pmatrix}^* \begin{pmatrix} D_{xx} & D_{xy} & D_{xz} \\ D_{yx} & D_{yy} & D_{yz} \\ D_{zx} & D_{zy} & D_{zz} \end{pmatrix} \begin{pmatrix} \frac{\partial W}{\partial x} \\ \frac{\partial W}{\partial y} \\ \frac{\partial W}{\partial z} \end{pmatrix} dV. \tag{3.9}$$

Since the combined dissipation matrix is positive semi–definite, the perturbation 'energy' is non-increasing thereby proving stability in the energy norm.

4 Semi–discrete equations

Using an unstructured grid of tetrahedral cells with W defined by linear interpolation between nodal values, the standard Galerkin spatial discretisation of the transformed p.d.e. is

$$M_G \frac{dW}{dt} + AW = -DW, \tag{4.1}$$

where

$$\begin{aligned} m_{G_{ij}} &= \int_\Omega N_i N_j \, I \, dV \\ a_{ij} &= \int_\Omega N_i \left(A_x \frac{\partial N_j}{\partial x} + A_y \frac{\partial N_j}{\partial y} + A_z \frac{\partial N_j}{\partial z} \right) dV \\ d_{ij} &= \int_\Omega \Bigg(D_{xx} \frac{\partial N_i}{\partial x}\frac{\partial N_j}{\partial x} + D_{xy} \frac{\partial N_i}{\partial x}\frac{\partial N_j}{\partial y} + D_{xz} \frac{\partial N_i}{\partial x}\frac{\partial N_j}{\partial z} \\ &\quad + D_{yx} \frac{\partial N_i}{\partial y}\frac{\partial N_j}{\partial x} + D_{yy} \frac{\partial N_i}{\partial y}\frac{\partial N_j}{\partial y} + D_{yz} \frac{\partial N_i}{\partial y}\frac{\partial N_j}{\partial z} \\ &\quad + D_{zx} \frac{\partial N_i}{\partial z}\frac{\partial N_j}{\partial x} + D_{zy} \frac{\partial N_i}{\partial z}\frac{\partial N_j}{\partial y} + D_{zz} \frac{\partial N_i}{\partial z}\frac{\partial N_j}{\partial z} \Bigg) \, dV. \end{aligned} \tag{4.2}$$

The vector W of discrete nodal variables has 5-component subvectors w_i at each node i. For a particular pair of nodes i, j, $m_{G_{ij}}$, a_{ij} and d_{ij} denote the corresponding 5×5 submatrices of the matrices M_G, A and D, respectively. N_i is the piecewise linear function which is equal to unity at node i and zero at all other nodes, and the viscosity parameters μ, λ and k within the dissipation matrices are defined to be constant on each tetrahedron.

An important point to note is that exactly the same semi-discrete equation would be obtained if one performed a Galerkin discretisation of the nonlinear Navier-Stokes equations expressed using the original conservative variables U, and then linearised the equations and transformed the variables to the symmetric variables W. Therefore, the stability analysis to be performed using the symmetric variables applies equally to actual computations performed using conservative variables.

A standard modification is to 'mass-lump' the matrix M_G, turning it into a diagonal matrix M with

$$m_{ii} = \sum_j m_{G_{ij}} = \int_\Omega N_i \, I \, dV = V_i \, I, \tag{4.3}$$

where V_i is the volume associated with node i, defined as one quarter of the sum of the volumes of the surrounding tetrahedra.

Another standard modification when interested in accelerating convergence to a steady-state solution, is to precondition the 'mass-lumped' matrix so that

$$m_{ii} = \frac{V_i}{\Delta t_i} \, I. \tag{4.4}$$

The objective of this preconditioning is to use local timesteps, Δt_i, which are larger in large computational cells than in small ones, so that fewer iterations of the fully-discrete equations will be needed to converge to the steady-state solution to within some specified tolerance.

The matrix A is antisymmetric since, integrating by parts,

$$\begin{aligned} a_{ij} &= -\int \left(A_x \frac{\partial N_i}{\partial x} N_j + A_y \frac{\partial N_i}{\partial y} N_j + A_z \frac{\partial N_i}{\partial z} N_j \right) dV \\ &= -\int N_j \left(A_x^T \frac{\partial N_i}{\partial x} + A_y^T \frac{\partial N_i}{\partial y} + A_z^T \frac{\partial N_i}{\partial z} \right) dV \\ &= -(a_{ji})^T. \end{aligned} \tag{4.5}$$

The matrix D is clearly symmetric. Furthermore, for any vector W,

$$W^* D W = \int_\Omega \begin{pmatrix} \frac{\partial W}{\partial x} \\ \frac{\partial W}{\partial y} \\ \frac{\partial W}{\partial z} \end{pmatrix}^* \begin{pmatrix} D_{xx} & D_{xy} & D_{xz} \\ D_{yx} & D_{yy} & D_{yz} \\ D_{zx} & D_{zy} & D_{zz} \end{pmatrix} \begin{pmatrix} \frac{\partial W}{\partial x} \\ \frac{\partial W}{\partial y} \\ \frac{\partial W}{\partial z} \end{pmatrix} dV, \tag{4.6}$$

where

$$\begin{aligned} \frac{\partial W}{\partial x} &= \sum_i \frac{\partial N_i}{\partial x} \, w_i \\ \frac{\partial W}{\partial y} &= \sum_i \frac{\partial N_i}{\partial y} \, w_i \\ \frac{\partial W}{\partial z} &= \sum_i \frac{\partial N_i}{\partial z} \, w_i. \end{aligned} \tag{4.7}$$

Since the combined dissipation matrix is positive semi-definite, it follows therefore that D is also positive semi-definite.

Defining the 'energy' for arbitrary complex W as either $E = \frac{1}{2}W^*M_GW$ or $E = \frac{1}{2}W^*MW$, depending whether or not mass-lumping is used,

$$\begin{aligned} \frac{dE}{dt} &= -\tfrac{1}{2}\left(W^*(A+D)W + W^*(A+D)^*W\right) \\ &= -\tfrac{1}{2}\left(W^*(A+D)W + W^*(-A+D)W\right) \\ &= -W^*DW \leq 0 \end{aligned} \tag{4.8}$$

and so the energy is non-increasing. Since both M_G and M are symmetric and positive definite this in turn implies stability for the semi-discrete equations.

Note that other discretisations of the Navier-Stokes equations will result in equations of the form,

$$M\frac{dU}{dt} = CU, \tag{4.9}$$

where M is a symmetric positive definite 'mass' matrix and C can be decomposed into its symmetric and anti–symmetric components,

$$C = -(A+D), \qquad A = -\tfrac{1}{2}(C-C^T), \qquad D = -\tfrac{1}{2}(C+C^T). \tag{4.10}$$

Although A is primarily due to the convective discretisation, in general it may also contain some terms due to the viscous discretisation. Similarly, D is primarily due to the viscous discretisation but may also contain some terms due to the numerical smoothing associated with the convective discretisation. D must still be positive semi–definite to ensure stability.

5 Fully discrete equations

Using Runge-Kutta time integration the fully discrete equations using one of the two diagonal mass matrices are

$$W^{(n+1)} = L(kM^{-1}C)\,W^{(n)} \tag{5.1}$$

where $L(z)$ is the Runge-Kutta polynomial with stability region S as defined in Section 2 and $C = -(A+D)$. As explained in Section 2, sufficient conditions for algebraic and generalised stability are that

$$\tau(kM^{-1/2}CM^{-1/2}) \subset S \tag{5.2}$$

where

$$\tau(kM^{-1/2}CM^{-1/2}) = \left\{ -k\,\frac{W^*M^{-1/2}CM^{-1/2}W}{W^*W} : W \neq 0 \right\}. \tag{5.3}$$

For unsteady calculations with the diagonal mass-lumped matrix, the aim is simply to find the largest k such that the constraint, Eq. (5.2), is satisfied.

For steady-state calculations using the pre-conditioned mass matrix, one uses a pseudo-timestep $k = 1$ and then the objective is to define the local timesteps Δt_i to be as large as possible, again subject to the sufficient stability constraint, Eq. (5.2).

The difficulty is that direct evaluation of $\tau(k\, M^{-1/2} C M^{-1/2})$ is not possible. Instead, a bounding set is constructed to enclose the numerical range and sufficient conditions are determined for this bounding set to lie inside S.

There are two choices of bounding set which are relatively easily constructed, a half-disk and a rectangle. The construction of the bounding half-disk starts with the observation that, when using L_2 norms,

$$\left| \frac{W^* M^{-1/2} C M^{-1/2} W}{W^* W} \right| \leq \| M^{-1/2} C M^{-1/2} \|. \tag{5.4}$$

Let the variable r be defined by

$$r = \max_i \left\{ m_i^{-1} \max \left\{ \sum_j \|c_{ij}\|, \sum_j \|c_{ji}\| \right\} \right\} \tag{5.5}$$

where

$$m_i = \begin{cases} V_i, & \text{mass-lumped matrix} \\ \dfrac{V_i}{\Delta t_i}, & \text{preconditioned mass-lumped matrix} \end{cases} \tag{5.6}$$

Considering an arbitrary vector V, with subvector v_i at each node i,

$$\begin{aligned} \|M^{-1/2} C M^{-1/2} V\|^2 &= \sum_i m_i^{-1} \left| \sum_j c_{ij} (m_j^{-1/2} v_j) \right|^2 \\ &\leq \sum_{i,j,k} m_i^{-1} \|c_{ij}\| m_j^{-1/2} \|v_j\| \|c_{ik}\| m_k^{-1/2} \|v_k\| \\ &\leq \sum_{i,j,k} m_i^{-1} m_j^{-1} \|v_j\|^2 \|c_{ij}\| \|c_{ik}\| \\ &\leq r \sum_{i,j} m_j^{-1} \|v_j\|^2 \|c_{ij}\| \\ &\leq r^2 \|V\|^2, \\ \implies \quad \|M^{-1/2} C M^{-1/2}\| &\leq r. \end{aligned} \tag{5.7}$$

The third line in the above derivation uses the inequality

$$m_j^{-1/2} \|v_j\| \; m_k^{-1/2} \|v_k\| \leq \tfrac{1}{2} \left(m_j^{-1} \|v_j\|^2 + m_k^{-1} \|v_k\|^2 \right), \tag{5.8}$$

followed by an interchange of subscripts to replace $m_k^{-1} \|v_k\|^2$ by $m_j^{-1} \|v_j\|^2$ given that $\|c_{ij}\| \|c_{ik}\|$ is symmetric in j and k.

Also, for an arbitrary vector W,

$$W^*CW + (W^*CW)^* = W^*(C+C^*)W = -2W^*DW \leq 0 \tag{5.9}$$

and so the real component of W^*CW must be zero or negative. Combined with the previous bound, this means that $\tau(kM^{-1/2}CM^{-1/2})$ must therefore lie in the half-disk

$$\{z = x+iy : x \leq 0, |z| \leq kr\}\,.$$

For unsteady calculations, the necessary and sufficient condition for the half-disk to lie inside S, and thus a sufficient condition for algebraic and generalised stability is

$$kr \leq r_c, \tag{5.10}$$

where r_c is the radius of the half-disk inscribing S, as defined and illustrated in Appendix A.

For preconditioned steady-state calculations with local timesteps, $k = 1$ and so the largest value for r for which the half-disk lies inside S is r_c. For each node i, Δt_i is then maximised subject to the definition of r by

$$\Delta t_i = \frac{r_c V_i}{\max\left\{\sum_j \|c_{ij}\|, \sum_j \|c_{ji}\|\right\}}. \tag{5.11}$$

These stability limits require knowledge of $\|c_{ij}\|$. Appendix C evaluates $\|a_{ij}\|$ exactly, using the fact that it is a symmetric matrix. Since $a_{ji} = -a_{ij}^T = -a_{ij}$, it follows that $\|a_{ji}\| = \|a_{ij}\|$. Appendix C also constructs a tight upper bound for $\|d_{ij}\|$ and $\|d_{ji}\|$. From these, an upper bound for $\|c_{ij}\|$ is obtained. Replacing $\|c_{ij}\|$ by this upper bound in the above stability limits gives a new slightly more restrictive sufficient stability condition which can be easily evaluated.

The rectangular bounding set is obtained by considering separately the numerical ranges of D and A. Since D is symmetric and positive semidefinite, the quantity
$x = -\dfrac{W^*M^{-1/2}DM^{-1/2}W}{W^*W}$ is real and negative with $-x_d \leq x \leq 0$ and x_d defined by

$$x_d = \max_i \left\{ m_i^{-1} \max\left\{\sum_j \|d_{ij}\|, \sum_j \|d_{ji}\|\right\}\right\}. \tag{5.12}$$

Similarly, since A is anti-symmetric, $y = i\,\dfrac{W^*M^{-1/2}AM^{-1/2}W}{W^*W}$ is real and $|y| \leq y_a$ with y_a defined by

$$y_a = \max_i \left\{ m_i^{-1} \max\left\{\sum_j \|a_{ij}\|, \sum_j \|a_{ji}\|\right\}\right\} = \max_i \left\{ m_i^{-1} \sum_j \|a_{ij}\|\right\}. \tag{5.13}$$

Thus the numerical range $\tau(kM^{-1/2}CM^{-1/2})$ must lie inside the rectangle

$$R = \{x+iy : -kx_d \leq x \leq 0,\ |y| \leq ky_a\}\,. \tag{5.14}$$

For unsteady calculations, a sufficient stability limit is obtained by requiring that $R \subset S$. If the boundary of S can be represented by $z = r\exp(i\theta)$ with $r(\theta)$ being a single-valued function for $\frac{\pi}{2} \leq \theta \leq \frac{3\pi}{2}$ then this can written as

$$k\sqrt{x_d^2 + y_a^2} \leq r(\theta), \qquad \tan(\theta) = -\frac{y_a}{x_d}. \tag{5.15}$$

For preconditioned steady-state calculations, we again let $k = 1$ and can then choose any rectangle R which inscribes S. Appendix A shows the particular example of a half-square for which $x_d = y_a$. The maximum local timestep Δt_i subject to the definitions of both x_D and y_A is then

$$\Delta t_i = \min\left\{\frac{x_d V_i}{\max\{\sum_j \|d_{ij}\|, \sum_j \|d_{ji}\|\}}, \frac{y_a V_i}{\sum_j \|a_{ij}\|}\right\}. \tag{5.16}$$

The final form of the stability limit is again obtained by using the results of Appendix C to evaluate $\|a_{ij}\|$ and place an upper bound on $\|d_{ij}\|$ and $\|d_{ji}\|$.

It is difficult to predict *a priori* which bounding set will give the least restrictive sufficient stability conditions. It depends in part on the particular Runge-Kutta method which is used. Appendix A shows that for some methods the inscribing half-disk almost contains the inscribing half-square and other rectangles lying inside S; in this case the half-disk sufficient stability conditions will probably be less restrictive. With other methods, the half-square almost contains the inscribing half-disk and for these the half-square stability conditions will probably be less restrictive.

6 Numerical experiments

A number of numerical experiments have been performed to test how close the predicted sufficient stability limits are to the necessary stability limits.

The calculations use a tetrahedral grid created from a uniform $10 \times 10 \times 10$ Cartesian grid by cutting each hexahedron into six tetrahedra. As indicated in Table 1, cases 1 and 3 use a grid based on a Cartesian grid with the same spacing in each direction, whereas for cases 2 and 4, the spacing in the y-direction is decreased by the specified amount. Periodic boundary conditions are used on all sides of the grid.

In all of the computations the mean flow is aligned with the x-axis and the Mach number is 0.5. Cases 1 and 2 are inviscid, while for cases 3 and 4 the cell Reynolds number $Re_{\Delta y} \equiv \frac{\rho u\, \Delta y}{\mu}$ is 1.0, the Prandtl number is 0.9 and $\lambda = -\frac{2}{3}\mu$.

Table 1: Parameters for four numerical test cases

	Grid stretching ratio	Cell Reynolds number
Case 1	1:1	∞
Case 2	10:1	∞
Case 3	1:1	1.0
Case 4	100:1	1.0

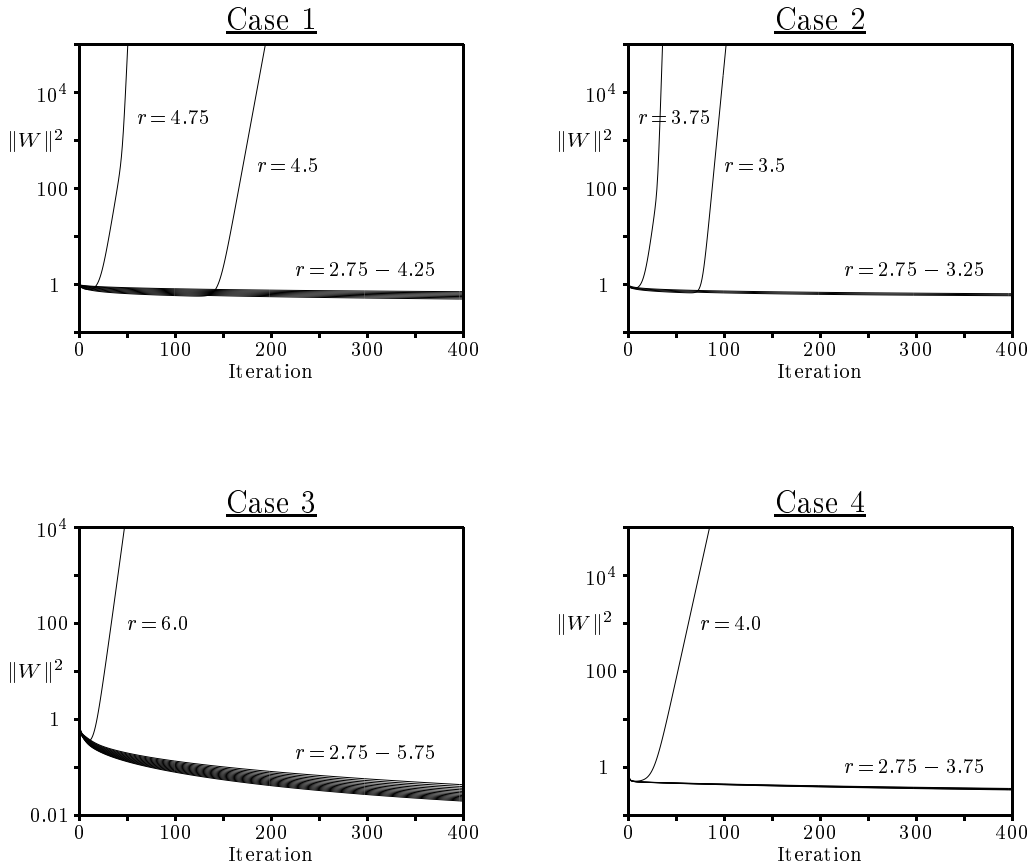

Figure 1: Evolution of energy in four test cases

The four-stage Runge-Kutta method described in Appendix A is used for the time-marching. The time-step is taken to be

$$\Delta t_i = \frac{rV_i}{\sum_j \|c_{ij}\|_{\text{bound}}}, \tag{6.1}$$

where $\|c_{ij}\|_{\text{bound}}$ denotes the upper bound for $\|c_{ij}\|$ derived in Appendix C. For each case, calculations were performed for a range of values of r starting with $r = 2.75$ and increasing in increments of 0.25. The initial conditions for the linear perturbation variables corresponded to a perturbation in pressure and density at one corner of the grid, and an equal but opposite perturbation in the centre. Figure 1 shows the evolution of the energy for the four cases, using a log scale for the energy.

Case 1 is the inviscid case on an unstretched grid. The theory for the rectangular bounding set predicts stability for $r < r_a$ and in this case $r_a \approx 2.828$. The results, however, show the actual stability boundary is at $r \approx 4.4$. Thus, the theory underpredicts the stability boundary by approximately 35%.

Case 2 is the inviscid case on a grid with a 10:1 stretching ratio. The theory again predicts stability for $r < r_a$. The results show the actual stability boundary to be at $r \approx 3.4$ so the sufficient stability theory now underpredicts the stability boundary by only 15%.

Both of these results are consistent with previous results by the author using energy analysis for two specific Runge-Kutta methods [6]. In that earlier work, the sufficient stability limit derived by energy analysis was compared to the necessary and sufficient Fourier stability limit for a uniform mesh. At worst, when the Mach number was zero and the grid spacing the same in each direction, the timestep limit from the energy analysis was 40% less than that from the Fourier analysis. At best, at high Mach numbers or on stretched grids, the two timestep limits were almost equal.

Note also that when the timestep is stable the results show a monotonic decrease in the energy. This is as predicted by the theory since in these two cases there is only the A matrix, and it is normal.

In case 3, the inviscid and viscous terms are equally important because of the unit cell Reynolds number. With the unstretched grid, this case is representative of turbulent flow calculations in combustors and wakes with very high levels of turbulent viscosity. The theory for the half-disk bounding set predicts stability for $r < r_c$, and for this Runge-Kutta method $r_c \approx 2.616$. The results show the actual stability boundary is at $r \approx 5.8$ so the theory underpredicts the stability boundary by 55%.

Case 4 is similar to case 3, but with a grid with a 100:1 stretching ratio representative of a boundary layer grid. In this case the actual stability boundary is at $r \approx 3.9$, and so the amount by which the theory underpredicts the stability boundary is reduced to 33%.

It is interesting that in these last two cases there is again a monotonic decrease in the energy when the timestep is stable. This is not predicted by the theory. It may be due to the particular choice of initial conditions, but attempts to find different initial conditions giving a transient energy growth were unsuccessful.

7 Conclusions

This paper has analysed the stability of one class of discretisations of the Navier-Stokes equations on a tetrahedral grid. The sufficient stability limits for both global and local timesteps are based on recent advances in numerical analysis. Numerical results demonstrate that in the worst case the sufficient stability limit can be less than half the necessary stability limit, but when the grid is highly stretched or the viscous terms are negligible the sufficient limit is much closer to the necessary limit.

Future research will consider the application of this method of stability analysis to other discretisations of the Euler and Navier-Stokes equations. Upwind approximations of the inviscid fluxes would be a particularly interesting topic for study. As indicated at the end of Section 4, this would change the definition of the dissipation matrix D, but the overall approach to the stability analysis would remain valid. It may also be possible to investigate the stability of different Navier-Stokes boundary condition implementations by incorporating these within the coupled system of o.d.e.'s.

Acknowledgements

I wish to thank Larry Wigton for stimulating this research and Eli Turkel, Eitan Tadmor, Bill Morton, Endré Süli, Nick Trefethen and Satish Reddy for their help with the numerical analysis literature on the stability of systems of o.d.e.'s with non-normal matrices, and for their valuable comments on the paper. The financial support of Rolls-Royce plc, DTI and EPSRC is gratefully acknowledged.

References

[1] L. Wigton. Personal communication, 1994.

[2] N.P. Weatherill, O. Hassan, M.J. Marchant, and D.L. Marcum. Adaptive inviscid flow solutions for aerospace geometries on efficiently generated unstructured tetrahedral meshes. AIAA Paper 93-3390, 1993.

[3] J. Peraire, J. Peiró, and K. Morgan. Finite element multigrid solution of Euler flows past installed aero-engines. *Comput. Mech.*, 11:433–451, 1993.

[4] R.D. Rausch, J.T. Batina, and H.T.Y. Yang. Three-dimensional time-marching aeroelastic analyses using an unstructured-grid Euler method. *AIAA J.*, 31(9):1626–1633, 1993.

[5] P. Crumpton and M.B. Giles. Aircraft computations using multigrid and an unstructured parallel library. AIAA Paper 95-0210, 1995.

[6] M.B. Giles. Energy stability analysis of multi-step methods on unstructured meshes. Technical Report TR-87-1, MIT Dept. of Aero. and Astro., 1987.

[7] R.D. Richtmyer and K.W. Morton. *Difference Methods for Initial-Value Problems*. Wiley-Interscience, 2nd edition, 1967. Reprint edn (1994) Krieger Publishing Company, Malabar.

[8] S.C. Reddy and L.N. Trefethen. Stability of the method of lines. *Numer. Math.*, 62:235–267, 1992.

[9] H.O. Kreiss and L. Wu. On the stability definition of difference approximations for the initial boundary value problem. *Appl. Num. Math.*, 12:213–227, 1993.

[10] J.L.M. van Dorsselaer and J.F.B. Kraaijevanger. Linear stability analysis in the numerical solution of initial value problems. *Acta Numer.*, pages 199–237, 1993.

[11] J.F.B.M. Kraaijevanger, H.W.J. Lenferink, and M.N. Spijker. Stepsize restrictions for stability in the numerical solution of ordinary and partial differential equations. *J. Comput. Appl. Math.*, 20:67–81, Nov 1987.

[12] H.W.J. Lenferink and M.N. Spijker. On the use of stability regions in the numerical analysis of initial value problems. *Math. Comp.*, 57(195):221–237, 1991.

[13] S.C. Reddy and L.N. Trefethen. Lax-stability of fully discrete spectral methods via stability regions and pseudo-eigenvalues. *Comput. Methods Appl. Mech. Engrg.*, 80:147–164, 1990.

[14] S.C. Reddy. *Pseudospectra of Operators and Discretization Matrices and an Application to Stability of the Method of Lines*. PhD thesis, Massachusetts Institute of Technology, Cambridge, Massachusetts 02139, 1991. Numerical Analysis Report 91-4.

[15] C. Lubich and O. Nevanlinna. On resolvent conditions and stability estimates. *BIT*, 31:293–313, 1991.

[16] B. Gustafsson and A. Sundström. Incompletely parabolic problems in fluid dynamics. *SIAM J. Appl. Math.*, 35(2):343–357, 1978.

[17] P. Dutt. Stable boundary conditions and difference schemes for the Navier–Stokes equations. *SIAM J. Numer. Anal.*, 25:245–267, 1988.

[18] S. Abarbanel and D. Gottlieb. Optimal time splitting for two- and three-dimensional Navier-Stokes equations with mixed derivatives. *Journal of Computational Physics*, 35:1–33, 1981.

Appendix A Runge-Kutta stability curves

An example of a Runge-Kutta type of approximation of the o.d.e.

$$\frac{du}{dt} = \lambda u, \tag{A.1}$$

is the following two-stage predictor-corrector method,

$$\begin{aligned} u^{(1)} &= u^n + k\lambda\, u^n \\ u^{n+1} &= u^n + k\lambda\, u^{(1)}. \end{aligned} \tag{A.2}$$

Combining these two equations gives

$$u^{n+1} = L(k\lambda)\; u^n, \tag{A.3}$$

where the Runge-Kutta polynomial function is $L(z) = 1 + z + z^2$. Figure 2a) shows the stability region S within which $|L| \leq 1$. It also shows the largest half-disk,

$$\{z = x + iy : x \leq 0, |z| \leq r_c\},$$

and the largest half-square,

$$\left\{z = x + iy : -\frac{r_s}{\sqrt{2}} \leq x \leq 0, |y| \leq \frac{r_s}{\sqrt{2}}\right\},$$

which lie inside S. If the boundary of S is defined as $z = r\exp(i\theta)$ then r_c and r_s can be defined as

$$r_c = \min_{\frac{\pi}{2} \leq \theta \leq \frac{3\pi}{2}} r(\theta), \qquad r_s = r(\tfrac{3}{4}\pi). \tag{A.4}$$

The values of r_c and r_s are listed to the right of the figure along with those of two other important parameters, $r_a = r(\frac{1}{2}\pi)$, which is the length of the positive imaginary axis segment within S, and $r_d = r(\pi)$, which is the length of the negative real axis segment within S. The importance of all four of these parameters is discussed in the main text in Section 5.

Figures 2b) and 2c) show the corresponding curves and data for two other popular multistage integration schemes.

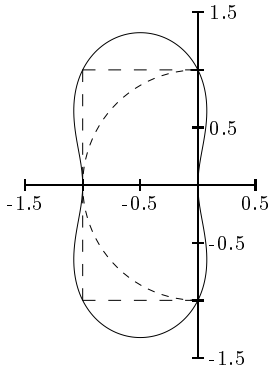

a) Predictor-corrector

$$
\begin{aligned}
u^{(1)} &= u^n + \lambda \Delta t\, u^n \\
u^{n+1} &= u^n + \lambda \Delta t\, u^{(1)} \\
r_c &= 1.0 \\
r_s &= 1.414 \\
r_a &= 1.0 \\
r_d &= 1.0
\end{aligned}
$$

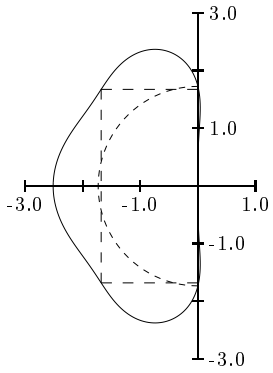

b) Three-stage scheme

$$
\begin{aligned}
u^{(1)} &= u^n + \tfrac{1}{3}\lambda \Delta t\, u^n \\
u^{(2)} &= u^n + \tfrac{1}{2}\lambda \Delta t\, u^{(1)} \\
u^{n+1} &= u^n + \lambda \Delta t\, u^{(2)} \\
r_c &= 1.731 \\
r_s &= 2.375 \\
r_a &= 1.731 \\
r_d &= 2.513
\end{aligned}
$$

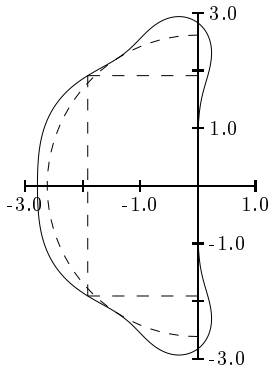

c) Four-stage scheme

$$
\begin{aligned}
u^{(1)} &= u^n + \tfrac{1}{4}\lambda \Delta t\, u^n \\
u^{(2)} &= u^n + \tfrac{1}{3}\lambda \Delta t\, u^{(1)} \\
u^{(3)} &= u^n + \tfrac{1}{2}\lambda \Delta t\, u^{(2)} \\
u^{n+1} &= u^n + \lambda \Delta t\, u^{(3)} \\
r_c &= 2.616 \\
r_s &= 2.704 \\
r_a &= 2.828 \\
r_d &= 2.785
\end{aligned}
$$

Figure 2: Stability boundary and inscribing half-disk and half-square for three Runge-Kutta methods

Appendix B vectors, matrices and positivity

Starting with the conservative form of the Navier-Stokes equations, the state vector and flux vectors are

$$
\begin{aligned}
U &= \begin{pmatrix} \rho \\ \rho u \\ \rho v \\ \rho w \\ \rho E \end{pmatrix}, \\
F_x &= \begin{pmatrix} \rho u & \\ \rho u^2 + p & -\tau_{xx} \\ \rho uv & -\tau_{yx} \\ \rho uw & -\tau_{zx} \\ \rho u(E + \frac{p}{\rho}) & -u\tau_{xx} - v\tau_{yw} - w\tau_{zx} + q_x \end{pmatrix} \\
F_y &= \begin{pmatrix} \rho v & \\ \rho uv & -\tau_{xy} \\ \rho v^2 + p & -\tau_{yy} \\ \rho vw & -\tau_{zy} \\ \rho v(E + \frac{p}{\rho}) & -u\tau_{xy} - v\tau_{yy} - w\tau_{zy} + q_y \end{pmatrix} \\
F_z &= \begin{pmatrix} \rho w & \\ \rho uw & -\tau_{xz} \\ \rho vw & -\tau_{yz} \\ \rho w^2 + p & -\tau_{zz} \\ \rho w(E + \frac{p}{\rho}) & -u\tau_{xz} - v\tau_{yz} - w\tau_{zz} + q_z \end{pmatrix}.
\end{aligned} \tag{B.1}
$$

ρ, u, v, w, p, E are the density, three Cartesian velocity components, pressure and total internal energy, respectively. To complete the system of equations requires an equation of state for an ideal gas,

$$p = \rho RT = (\gamma - 1)\,\rho\,(E - \tfrac{1}{2}(u^2 + v^2 + w^2)), \tag{B.2}$$

in which R, T, γ are the gas constant, temperature and uniform specific heat ratio, respectively, as well as equations defining the heat fluxes,

$$q_x = -k\frac{\partial T}{\partial x}, \quad q_y = -k\frac{\partial T}{\partial y}, \quad q_z = -k\frac{\partial T}{\partial z}, \tag{B.3}$$

and the viscous stress terms,

$$\begin{aligned}
\tau_{xx} &= 2\mu\frac{\partial u}{\partial x} + \lambda\left(\frac{\partial u}{\partial x} + \frac{\partial v}{\partial y} + \frac{\partial w}{\partial z}\right), \qquad \tau_{xy} = \tau_{yx} = \mu\left(\frac{\partial u}{\partial y} + \frac{\partial v}{\partial x}\right), \\
\tau_{yy} &= 2\mu\frac{\partial v}{\partial y} + \lambda\left(\frac{\partial u}{\partial x} + \frac{\partial v}{\partial y} + \frac{\partial w}{\partial z}\right), \qquad \tau_{xz} = \tau_{zx} = \mu\left(\frac{\partial u}{\partial z} + \frac{\partial w}{\partial x}\right), \\
\tau_{zz} &= 2\mu\frac{\partial w}{\partial z} + \lambda\left(\frac{\partial u}{\partial x} + \frac{\partial v}{\partial y} + \frac{\partial w}{\partial z}\right), \qquad \tau_{yz} = \tau_{zy} = \mu\left(\frac{\partial v}{\partial z} + \frac{\partial w}{\partial y}\right). \quad \text{(B.4)}
\end{aligned}$$

The transformation between the conservative variables and the symmetrising variables of Gustafsson and Sundstrom [16] and Abarbanel and Gottlieb [18], $(\frac{1}{\sqrt{\gamma}}\frac{c}{\rho}\,\widetilde{\rho},\ \widetilde{u},\ \widetilde{v},\ \widetilde{w},\ \frac{1}{\sqrt{\gamma(\gamma-1)}}\frac{c}{T}\,\widetilde{T})^T$, is accomplished by the matrix

$$S = \begin{pmatrix}
\sqrt{\gamma}\,\frac{\rho}{c} & 0 & 0 & 0 & 0 \\
\sqrt{\gamma}\,\frac{\rho u}{c} & \rho & 0 & 0 & 0 \\
\sqrt{\gamma}\,\frac{\rho v}{c} & 0 & \rho & 0 & 0 \\
\sqrt{\gamma}\,\frac{\rho w}{c} & 0 & 0 & \rho & 0 \\
\sqrt{\gamma}\,\frac{\rho E}{c} & \rho u & \rho v & \rho w & \sqrt{\frac{\gamma}{\gamma-1}}\,\frac{p}{c}
\end{pmatrix}. \quad \text{(B.5)}$$

The linearised, transformed equations are

$$\begin{aligned}
\frac{\partial W}{\partial t} + A_x\frac{\partial W}{\partial x} + A_y\frac{\partial W}{\partial y} + A_z\frac{\partial W}{\partial z} \;=\; & \frac{\partial}{\partial x}\left(D_{xx}\frac{\partial W}{\partial x} + D_{xy}\frac{\partial W}{\partial y} + D_{xz}\frac{\partial W}{\partial z}\right) \\
+\; & \frac{\partial}{\partial y}\left(D_{yx}\frac{\partial W}{\partial x} + D_{yy}\frac{\partial W}{\partial y} + D_{yz}\frac{\partial W}{\partial z}\right) \\
+\; & \frac{\partial}{\partial z}\left(D_{zx}\frac{\partial W}{\partial x} + D_{zy}\frac{\partial W}{\partial y} + D_{zz}\frac{\partial W}{\partial z}\right) \quad \text{(B.6)}
\end{aligned}$$

where

$$A_x = \begin{pmatrix}
u & \frac{1}{\sqrt{\gamma}}\,c & 0 & 0 & 0 \\
\frac{1}{\sqrt{\gamma}}\,c & u & 0 & 0 & \sqrt{\frac{\gamma-1}{\gamma}}\,c \\
0 & 0 & u & 0 & 0 \\
0 & 0 & 0 & u & 0 \\
0 & \sqrt{\frac{\gamma-1}{\gamma}}\,c & 0 & 0 & u
\end{pmatrix},$$

$$A_y = \begin{pmatrix}
v & 0 & \frac{1}{\sqrt{\gamma}}\,c & 0 & 0 \\
0 & v & 0 & 0 & 0 \\
\frac{1}{\sqrt{\gamma}}\,c & 0 & v & 0 & \sqrt{\frac{\gamma-1}{\gamma}}\,c \\
0 & 0 & 0 & v & 0 \\
0 & 0 & \sqrt{\frac{\gamma-1}{\gamma}}\,c & 0 & v
\end{pmatrix},$$

$$A_z = \begin{pmatrix} w & 0 & 0 & \frac{1}{\sqrt{\gamma}}\,c & 0 \\ 0 & w & 0 & 0 & 0 \\ 0 & 0 & w & 0 & 0 \\ \frac{1}{\sqrt{\gamma}}\,c & 0 & 0 & w & \sqrt{\frac{\gamma-1}{\gamma}}\,c \\ 0 & 0 & 0 & \sqrt{\frac{\gamma-1}{\gamma}}\,c & w \end{pmatrix}, \tag{B.7}$$

and

$$D_{xx} = \begin{pmatrix} 0 & 0 & 0 & 0 & 0 \\ 0 & \frac{2\mu+\lambda}{\rho} & 0 & 0 & 0 \\ 0 & 0 & \frac{\mu}{\rho} & 0 & 0 \\ 0 & 0 & 0 & \frac{\mu}{\rho} & 0 \\ 0 & 0 & 0 & 0 & \frac{\gamma\mu}{\mathrm{Pr}\,\rho} \end{pmatrix}, \qquad D_{xy} = D_{yx}^T = \begin{pmatrix} 0 & 0 & 0 & 0 & 0 \\ 0 & 0 & \frac{\lambda}{\rho} & 0 & 0 \\ 0 & \frac{\mu}{\rho} & 0 & 0 & 0 \\ 0 & 0 & 0 & 0 & 0 \\ 0 & 0 & 0 & 0 & 0 \end{pmatrix},$$

$$D_{yy} = \begin{pmatrix} 0 & 0 & 0 & 0 & 0 \\ 0 & \frac{\mu}{\rho} & 0 & 0 & 0 \\ 0 & 0 & \frac{2\mu+\lambda}{\rho} & 0 & 0 \\ 0 & 0 & 0 & \frac{\mu}{\rho} & 0 \\ 0 & 0 & 0 & 0 & \frac{\gamma\mu}{\mathrm{Pr}\,\rho} \end{pmatrix}, \qquad D_{xz} = D_{zx}^T = \begin{pmatrix} 0 & 0 & 0 & 0 & 0 \\ 0 & 0 & 0 & \frac{\lambda}{\rho} & 0 \\ 0 & 0 & 0 & 0 & 0 \\ 0 & \frac{\mu}{\rho} & 0 & 0 & 0 \\ 0 & 0 & 0 & 0 & 0 \end{pmatrix},$$

$$D_{zz} = \begin{pmatrix} 0 & 0 & 0 & 0 & 0 \\ 0 & \frac{\mu}{\rho} & 0 & 0 & 0 \\ 0 & 0 & \frac{\mu}{\rho} & 0 & 0 \\ 0 & 0 & 0 & \frac{2\mu+\lambda}{\rho} & 0 \\ 0 & 0 & 0 & 0 & \frac{\gamma\mu}{\mathrm{Pr}\,\rho} \end{pmatrix}, \qquad D_{yz} = D_{zy}^T = \begin{pmatrix} 0 & 0 & 0 & 0 & 0 \\ 0 & 0 & 0 & 0 & 0 \\ 0 & 0 & 0 & \frac{\lambda}{\rho} & 0 \\ 0 & 0 & \frac{\mu}{\rho} & 0 & 0 \\ 0 & 0 & 0 & 0 & 0 \end{pmatrix}. \tag{B.8}$$

The Prandtl number is defined as

$$\mathrm{Pr} = \frac{\mu c_p}{k} = \frac{\gamma\mu R}{(\gamma-1)k}, \tag{B.9}$$

but is not assumed to be uniform since λ and k in general represent combinations of laminar and turbulent viscosities, each with their own Prandtl number.

An important feature of the transformed equations is that the combined dissipation matrix,

$$\begin{pmatrix} D_{xx} & D_{xy} & D_{xz} \\ D_{yx} & D_{yy} & D_{yz} \\ D_{zx} & D_{zy} & D_{zz} \end{pmatrix}$$

is both symmetric and positive semi-definite. The symmetry is clear from the above definitions of the component matrices, and the positivity comes from noting that

$$
\begin{aligned}
x^T \begin{pmatrix} D_{xx} & D_{xy} & D_{xz} \\ D_{yx} & D_{yy} & D_{yz} \\ D_{zx} & D_{zy} & D_{zz} \end{pmatrix} x &= \frac{\mu}{\rho}(x_3+x_7)^2 + \frac{\mu}{\rho}(x_4+x_{12})^2 + \frac{\mu}{\rho}(x_9+x_{13})^2 \\
&+ \frac{1}{\rho} \begin{pmatrix} x_2 \\ x_8 \\ x_{14} \end{pmatrix}^T \begin{pmatrix} 2\mu+\lambda & \lambda & \lambda \\ \lambda & 2\mu+\lambda & \lambda \\ \lambda & \lambda & 2\mu+\lambda \end{pmatrix} \begin{pmatrix} x_2 \\ x_8 \\ x_{14} \end{pmatrix} \\
&+ \frac{\gamma\mu}{\mathrm{Pr}\rho}(x_5^2 + x_{10}^2 + x_{15}^2). \qquad \text{(B.10)}
\end{aligned}
$$

The eigenvalues of

$$
\begin{pmatrix} 2\mu+\lambda & \lambda & \lambda \\ \lambda & 2\mu+\lambda & \lambda \\ \lambda & \lambda & 2\mu+\lambda \end{pmatrix}
$$

are $2\mu, 2\mu, 2\mu+3\lambda$ and hence the combined dissipation matrix is positive semi-definite provided $\mu \geq 0, \quad 2\mu+3\lambda \geq 0$ and $k \geq 0$.

Appendix C L_2 norms of component matrices

Defining

$$\int_\Omega N_i \nabla N_j \, dV = S\,\vec{n}, \tag{C.1}$$

then

$$\begin{aligned} a_{ij} &= S\,(n_x A_x + n_y A_y + n_z A_z) \\ &= S \begin{pmatrix} \vec{u}.\vec{n} & \frac{1}{\sqrt{\gamma}} c n_x & \frac{1}{\sqrt{\gamma}} c n_y & \frac{1}{\sqrt{\gamma}} c n_z & 0 \\ \frac{1}{\sqrt{\gamma}} c n_x & \vec{u}.\vec{n} & 0 & 0 & \sqrt{\frac{\gamma-1}{\gamma}} c n_x \\ \frac{1}{\sqrt{\gamma}} c n_y & 0 & \vec{u}.\vec{n} & 0 & \sqrt{\frac{\gamma-1}{\gamma}} c n_y \\ \frac{1}{\sqrt{\gamma}} c n_z & 0 & 0 & \vec{u}.\vec{n} & \sqrt{\frac{\gamma-1}{\gamma}} c n_z \\ 0 & \sqrt{\frac{\gamma-1}{\gamma}} c n_x & \sqrt{\frac{\gamma-1}{\gamma}} c n_y & \sqrt{\frac{\gamma-1}{\gamma}} c n_z & \vec{u}.\vec{n} \end{pmatrix}. \end{aligned} \tag{C.2}$$

Three of the eigenvalues of $S^{-1}a_{ij}$ are equal to $\vec{u}.\vec{n}$ and the other two are $\vec{u}.\vec{n} \pm c$, and so

$$\|a_{ij}\| = S\,(|\vec{u}.\vec{n}| + c), \tag{C.3}$$

since the L_2 norm of a symmetric matrix is the magnitude of the largest eigenvalue.

The quantity $S\vec{n}$ can be interpreted geometrically. First note that ∇N_j is non-zero only on tetrahedra surrounding node j, and that on such a tetrahedron, labelled σ,

$$\nabla N_j = \frac{1}{3V^\sigma} \vec{S}_j^\sigma \tag{C.4}$$

where $\vec{S}_j^\sigma$ is the inward-pointing area vector of the face of σ opposite node j, and V^σ is the volume of the tetrahedron. Summing over all tetrahedra for which both i and j are corner nodes, gives

$$S\,\vec{n} = \frac{1}{12} \sum_\sigma \vec{S}_j^\sigma \tag{C.5}$$

Define d_{ij}^σ to be the contribution to d_{ij} from the integration over tetrahedron σ. Therefore,

$$d_{ij} = \sum_\sigma d_{ij}^\sigma \quad \Longrightarrow \quad \|d_{ij}\| \le \sum_\sigma \|d_{ij}^\sigma\| \tag{C.6}$$

where again the summation is over tetrahedra common to both i and j. On

tetrahedron σ, ∇N_i and ∇N_j are both uniform and so

$$d_{ij}^{\sigma} = V^{\sigma} \begin{pmatrix} 0 & 0 & 0 & 0 & 0 \\ 0 & \frac{\mu+\lambda}{\rho}\frac{\partial N_i}{\partial x}\frac{\partial N_j}{\partial x} + \frac{\mu}{\rho}\nabla N_i \cdot \nabla N_j & \frac{\lambda}{\rho}\frac{\partial N_i}{\partial x}\frac{\partial N_j}{\partial y} + \frac{\mu}{\rho}\frac{\partial N_i}{\partial y}\frac{\partial N_j}{\partial x} & \frac{\lambda}{\rho}\frac{\partial N_i}{\partial x}\frac{\partial N_j}{\partial z} + \frac{\mu}{\rho}\frac{\partial N_i}{\partial z}\frac{\partial N_j}{\partial x} & 0 \\ 0 & \frac{\lambda}{\rho}\frac{\partial N_i}{\partial y}\frac{\partial N_j}{\partial x} + \frac{\mu}{\rho}\frac{\partial N_i}{\partial x}\frac{\partial N_j}{\partial y} & \frac{\mu+\lambda}{\rho}\frac{\partial N_i}{\partial y}\frac{\partial N_j}{\partial y} + \frac{\mu}{\rho}\nabla N_i \cdot \nabla N_j & \frac{\lambda}{\rho}\frac{\partial N_i}{\partial y}\frac{\partial N_j}{\partial z} + \frac{\mu}{\rho}\frac{\partial N_i}{\partial z}\frac{\partial N_j}{\partial y} & 0 \\ 0 & \frac{\lambda}{\rho}\frac{\partial N_i}{\partial z}\frac{\partial N_j}{\partial x} + \frac{\mu}{\rho}\frac{\partial N_i}{\partial x}\frac{\partial N_j}{\partial z} & \frac{\lambda}{\rho}\frac{\partial N_i}{\partial z}\frac{\partial N_j}{\partial y} + \frac{\mu}{\rho}\frac{\partial N_i}{\partial y}\frac{\partial N_j}{\partial z} & \frac{\mu+\lambda}{\rho}\frac{\partial N_i}{\partial z}\frac{\partial N_j}{\partial z} + \frac{\mu}{\rho}\nabla N_i \cdot \nabla N_j & 0 \\ 0 & 0 & 0 & 0 & \frac{\gamma\mu}{\mathrm{Pr}\rho}\nabla N_i \cdot \nabla N_j \end{pmatrix} \tag{C.7}$$

Hence,

$$\|d_{ij}^{\sigma}\| \leq V^{\sigma} \max\left\{ \frac{2\mu+\lambda}{\rho} |\nabla N_i|\,|\nabla N_j|, \frac{\gamma\mu}{\mathrm{Pr}\rho} |\nabla N_i \cdot \nabla N_j| \right\} \tag{C.8}$$

which can be re-expressed using the values for ∇N_i and ∇N_j as

$$\|d_{ij}^{\sigma}\| \leq \frac{1}{9V^{\sigma}} \max\left\{ \frac{2\mu+\lambda}{\rho} |\vec{S}_i^{\sigma}|\,|\vec{S}_j^{\sigma}|, \frac{\gamma\mu}{\mathrm{Pr}\rho} |\vec{S}_i^{\sigma} \cdot \vec{S}_j^{\sigma}| \right\}, \tag{C.9}$$

where $\vec{S}_i^{\sigma}$ and $\vec{S}_j^{\sigma}$ are as defined previously. Note that the upper bound on the right-hand-side of Eq. (C.9) is unchanged if i and j are interchanged, and so it is also an upper bound for $\|d_{ji}^{\sigma}\|$. Hence,

$$\max\{\|d_{ij}\|, \|d_{ji}\|\} \leq \sum_{\sigma} \frac{1}{9V^{\sigma}} \max\left\{ \frac{2\mu+\lambda}{\rho} |\vec{S}_i^{\sigma}|\,|\vec{S}_j^{\sigma}|, \frac{\gamma\mu}{\mathrm{Pr}\rho} |\vec{S}_i^{\sigma} \cdot \vec{S}_j^{\sigma}| \right\}. \tag{C.10}$$

The exact value for $\|a_{ij}\|$ and the upper bounds for $\|d_{ij}\|, \|d_{ji}\|$ can then be combined by the triangle inequality,

$$\|c_{ij}\| = \|a_{ij} + d_{ij}\| \leq \|a_{ij}\| + \|d_{ij}\|, \tag{C.11}$$

to get upper bounds for $\|c_{ij}\|$ and $\|c_{ji}\|$ for use in the sufficient stability limits derived in Section 5 in the main text.